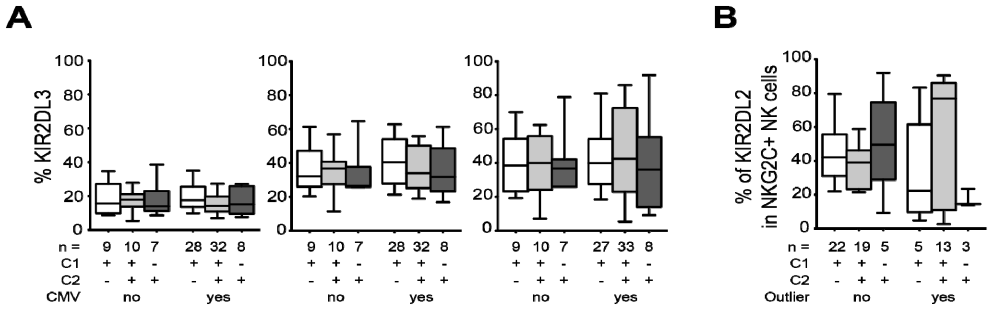

Supplementary Figure 1. Effect of HLA-C on KIR2DL2/S2 expression. (A) The effect of HCMV-seropositivity and HLA class I (C1/C1 white bars, C1/C2 light grey bars, and C2/C2 dark grey bars) on KIR2DL2 expression was examined in distinct NK cells subsets: $NKG2A^{+}$ (left), $NKG2C^{-}NKG2A^{-}$ (center) and $NKG2C^{+}$ (right). (B) The effect of HLA class I on KIR2DL2 expression in CMV-seropositive individuals with and without evidence of NK cell expansion.

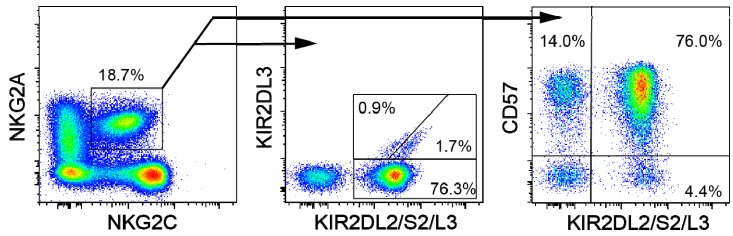

Supplementary Figure 2. Characteristics of the NKG2A$^+$ outlier. Shown is the KIR repertoire of the single outlier found in the NKG2A$^+$ compartment with a differentiated phenotype. This outlier co-expressed NKG2C and had a biased expression of KIR2DL2. The differentiated phenotype is illustrated by the high expression of CD57.

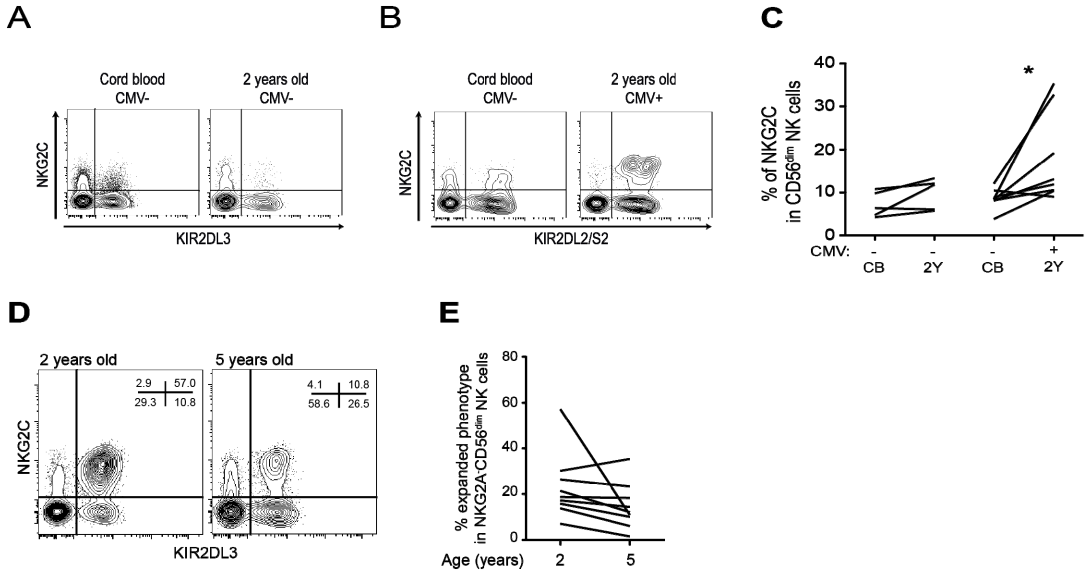

Supplementary Figure 3. Dynamics of the NKG2C-driven NK cell expansions in early life. Density plots show representative stainings of NKG2C and relevant KIR in cord blood and in matched longitudinal samples from children without (A) and with (B) evidence of latent CMV infection at the age of 2 years. **(**C) Summary of dynamics in the NKG2C^{+} compartment between the ages 0 and 2 years in HCMV seronegative (left, n=5) and seropositive (right, n=8) children. Expansions were defined as NKG2C^{+}KIR^{+}CD161^{-}. Wilcoxon non-parametric paired test. *p<0.05. (D) The FACS plot shows an example of a child with contraction of the expanded NK cell subsets between the ages two and five years. (E) Summary of dynamics in the NKG2C^{+} compartment between the ages two and five years (n=9). Expansions were defined as NKG2C^{+}KIR^{+}CD161^{-}.

Supplementary methods

Selection/exclusion of donors

Among the 204 healthy individuals, 14 expressed the KIR2DL3*005 allele, which crossreacts with the EB6 clone but is not recognized by the 180701 clone (Falco et al., 2010). Five of these donors were KIR2DS1$^+$ and/or KIR2DL2/S2$^+$ and were excluded because KIR2DL3*005 expression could not be discriminated from KIR2DS1 and/or KIR2DL2/S2. Four of the five excluded donors were CMV-seronegative. Hence 199 donors were included out of which 149 were CMV-seropositive. The presence of the homozygous deletion of the NKG2C gene was assessed by PCR as previously described.[1] In the present cohort, five donors were homozygous for a deletion of the NKG2C gene and were not taken into account in the analysis of the NKG2C$^+$ compartment.

Virus serology

An indirect enzyme immunoassay (EIA) to detect IgG antibodies against herpes simplex virus (HSV)-1 and HSV-2 was used as previously described [2]. Patient sera were incubated in microtiterstrips coated with recombinant gG-1/gG-2 antigens. Thereafter, peroxidase labeled anti-human IgG was added, which binds to human HSV-1/HSV-2 IgG-antibodies. The antigen-antibody complex was then measured by spectrophotometry. Measurements of antibodies against Epstein-Barr virus (EBV) were made using Enzygnost® Anti-EBV/IgG (Siemens) [3]. Cytomegalovirus (CMV) serology was determined using an ELISA-based assay on plasma obtained during sample preparation. Purified nuclear CMV antigen (AD 169) was used and the cut-off level for seropositivity was an absorbance of $\geq$0.2 at a dilution of 1/100. Varicellae-zoster virus (VZV) serology was determined using Enzygnost® Anti-VZV/IgG (Siemens). IgG antibodies against VZV were added to VZV antigens adsorbed to the plastic in wells of microstrips. A peroxidase labeled anti-human IgG antibody was added and the absorbance of a Tetramethylbenzidine (TMB) substrate was read on a spectrophotometer. In the children cohort, CMV serology was determined at each time point of the sampling as previously described [4].

Antibodies, custom conjugates, and instrument details

The following antibodies and fluorochromes were used (clone names are given within parentheses): KIR2DL3-FITC (180701), NKG2A-APC (Z199), KIR3DL1-AlexaFluor 700 (DX9), CD57-Pacific blue (NC1), CD14-Horizon-V500 (M5E2), CD19-Horizon-V500 (HIB19), KIR2DS4-Qdot.585 (179315), KIR3DL2-biotin (DX31), KIR2DL1-Qdot.705 (143211), NKG2C-PE (134522), CD56-ECD (N901), CD3-PE.Cy5 (UCHT1), KIR2DL2/S2/L3-PE.Cy5.5 (GL183), KIR2DL1/S1-PE.Cy7 (EB6), CD2-Pacific blue (TS1/8), NKp30-Alexa Fluor 647 (P30-15), CD161-APC (DX12), Siglec-9-PE (K8), CD7-AlexaFluor 647 (CD7-6B7). Biotin-conjugated antibodies were visualized using streptavidin-Qdot 605. Importantly, for a good separation of KIR2DL1 and KIR2DS1, a two-step staining was performed as previously described [5]. KIR2DS4 and KIR2DL1 were conjugated in house with Qdot 585 and Qdot 705 conjugation kits (Invitrogen), respectively. The BD-LSR Fortessa instrument was equipped with a 100 mW 405 nm laser, a 100 mW 488 nm laser, a 50 mW 561 nm laser, and a 40 mW 639 nm laser.

Functional assays

For measurements of degranulation (CD107a), PBMCs (10^6 cells) were mixed with rituximab (1μg/mL) and RAJI cells at a ratio of 10:1 in U-bottomed 96-well plates, centrifuged at 300 rpm for 3 minutes, and incubated for 2 hours at 37°C at 5% CO_2. Anti-CD107a-APC.Cy7 (H4A3) was added prior the start of the assay. After incubation, cells were harvested by centrifugation, surface stained with appropriate antibody combinations to identify KIR subsets, fixed (Fixation & Permeabilization Buffers, eBioscience) and analyzed by flow cytometry. For assessment of intracellular cytokines, PBMCs (10^6 cells) were incubated 16 hours at 37°C at 5% CO2 with 10 ng/ml IL-12 and 100 ng/ml IL-18 in U-bottomed 96-well plates. After incubation, cells were harvested by centrifugation, then surface-stained with appropriate antibody combinations to identify KIR subsets. Cells were subsequently fixed and permeabilized (Fix/Perm, eBioscience), stained with anti-IFN-γ-AF700 (B27) and analyzed by flow cytometry. To measure NK cell proliferation, NK cells were negatively isolated from PBMC using the NK cell isolation kit (Miltenyi) and labeled with CellTrace CFSE (Invitrogen). 10^6 labeled NK cells were cultured in 20 ng/mL IL-15 in 96-well round bottom plates in the presence or absence of 10^5 221.wt or 221.AEH target cells. Medium and IL-15 were replaced every two to three days. After 7 and 14 days of incubation cells were harvested, stained for appropriate extracellular markers, fixed and analyzed by flow cytometry. NK cell proliferation was determined by measuring CFSE dilution.

Statistical identification of outliers

Chauvenet's criterion can be used to identify outliers in a Gaussian distribution and is commonly applied to eliminate erroneous data points. Here, instead those data points were carefully assessed, and many outliers proved to represent cellular expansions. To minimize the number of false-positive outliers among subsets of very low frequencies, not likely to represent NK cell expansions, two additional criteria were defined: The outliers should represent (i) at least 5% of the total NK cell population and ii) at least 20% of the subset from which they originated ($NKG2A^+$, $NKG2A^-$ $NKG2C^-$, $NKG2A^+$). Data were analyzed using Octave.

References

1. Miyashita R, Tsuchiya N, Hikami K, et al. Molecular genetic analyses of human NKG2C (KLRC2) gene deletion. *Int Immunol*. 2004;16(1):163-168.
2. Ashley RL. Performance and use of HSV type-specific serology test kits. *Herpes*. 2002;9(2):38-45.
3. Kleines M, Scheithauer S, Ritter K, Hausler M. Sensitivity of the Enzygnost anti-EBV/IgG for the determination of the Epstein-Barr virus immune status in pediatric patients. *Diagn Microbiol Infect Dis*. 2006;55(3):247-249.
4. Nilsson C, Linde A, Montgomery SM, et al. Does early EBV infection protect against IgE sensitization? *J Allergy Clin Immunol*. 2005;116(2):438-444.
5. Fauriat C, Ivarsson MA, Ljunggren HG, Malmberg KJ, Michaelsson J. Education of human natural killer cells by activating killer cell immunoglobulin-like receptors. *Blood*. 2010;115(6):1166-1174.

Supplementary table 2. Characteristics of NKG2C$^-$NKG2A$^-$ false-positive outliers

						KIR3DL1		KIR genotyping																
Donor	HLA-C	Phenotype of Outlier	CMV	EBV	Haplotype	86 or 182 substitution*	Expression detected	3DL3	2DS2#	2DL2#	2DL3#	2DP1	2DL1#	3DP1	2DL4	3DL1#	3DS1	2DL5	2DS3	2DS5	2DS1#	2DS4Wt#,&	2DS4Del#,§	3DL2	KIR genes detected by flow cytometry
#077	C1/C2	2DL1+	+	+	A/A	Yes	Yes	1	0	0	1	1	1	1	1	1	0	0	0	0	0	0	1	1	4/4
#090	C1/C2	2DL2+	+	+	B/B	No	No	1	1	1	0	0	0	1	1	0	1	1	0	1	1	0	0	1	4/4
#099**	C1/C2	2DL3+ 2DL3+3DL2+	-	+	A/A	Yes	No	1	0	0	1	1	1	1	1	1	0	0	0	0	0	0	1	1	3/4
#122**	C1/C2	2DL2+3DL2+ 2DL2+3DL1+ 3DL2+	-	+	B/B	No	Yes	1	1	1	0	0	0	1	1	1	0	0	0	0	0	0	1	1	4/4
#140	C1/C2	2DL3+	+	+	A/B	Yes	No	1	0	0	1	1	1	1	1	1	1	1	0	1	1	0	1	1	4/5
#149	C1/C1	2DL3+	+	+	A/A	Yes	Yes	1	0	0	1	1	1	1	1	1	0	0	0	0	0	0	1	1	4/4
#170	C1/C1	2DL3+	+	+	A/A	Yes	No	1	0	0	1	1	1	1	1	1	0	0	0	0	0	0	1	1	3/4
#200	C2/C2	2DL1+	+	+	A/A	Yes	Yes	1	0	0	1	1	1	1	1	1	0	0	0	0	0	0	1	1	4/4

* Substitutions at positions 86 in Ig Domain 0 and 182 in Ig Domain 1 of KIR3DL1 were shown to result in poor or absent KIR3DL1 expression (Pando M.J. *et al.*, Journal of Immunology, 2003)
** Donors #099 and #122 had two outliers each in the NKG2C-NKG2A- compartment
# KIR genes product detected by flow cytometry (KIR2DS2, KIR2DL2, KIR2DL3, KIR2DL1, KIR3DL1, KIR2DS1, KIR2DS4 and KIR3DL2).
& KIR2DS4^{wt}: full length KIR2DS4 alleles, expressed on the cell surface.
§ KIR2DS4^{del}: KIR2DS4 alleles carrying a deletion resulting in an absence of expression on the cell surface.

Supplementary table 3. Characteristics of NKG2C$^-$ NK cell expansions

Donor	CMV	Expansion phenotype		Self-KIR status	KIR Haplo-types	KIR-Ligand genotyping			
		Act. KIR	Inhib. KIR			HLA-C1	HLA-C2	HLA-Bw4	HLA-A*03/*11
#033	+	2DS2	2DL1	Y	B3,B5/ A2,B8	+	+	+	-
#046	+	3DS1	3DL2	N	A2,B3	+	+	-	-
#050	+	3DS1	2DL3 / 3DL2	Y	A1,B3	+	+	-	-
#059	+	3DS1	2DL3 / 3DL2	Y	A1,B3	+	-	-	-
#069	+	2DS4	3DL2	N	A2,B4/ A1,B5	+	-	+	-
#154	+	2DS2	3DL1	N	A1,B4	+	-	-	+
#177	+	2DS4	2DL3 / 3DL2	Y	A1,B20/ A2,B16	+	-	+	-
#198	+	2DS2	3DL2	N	B5,B13	+	-	+	-

KIR haplotypes (derived from http://www.bioinformatics.cimr.cam.ac.uk/haplotypes/; Jiang et al. Gen Res 2012):
A1: 3DL3-2DL3-2DP1-2DL1-3DP1-2DL4-3DL1-2DS4d-3DL2
A2: 3DL3-2DL3-2DP1-2DL1-3DP1-2DL4-3DL1-2DS4f-3DL2
B3: 3DL3-2DL3-2DP1-2DL1-3DP1-2DL4-3DS1-2DL5-2DS5-2DS1-3DL2
B4: 3DL3-2DS2-2DL2-3DP1-2DL4-3DL1-2DS4d-3DL2
B5: 3DL3-2DS2-2DL2-3DP1-2DL4-3DL1-2DS4f-3DL2
B8: 3DL3-2DS2-2DL2-3DP1-2DL4-3DS1-2DL5-2DS5-2DS1-3DL2
B9: 3DL3-2DS2-2DL2-2DL5-2DP1-2DL1-3DP1-2DL4-3DS1-2DL5-2DS3-2DS1-3DL2
B13: 3DL3-2DS2-2DL2-2DP1-2DL1-3DP1(2 copies)-2DL4(2 copies)-3DL1-3DS1-2DL5-2DS3-2DS4f-3DL2
B16: 3DL3-2DL3-2DP1-2DL1-3DP1(2 copies)-2DL4(2 copies)-3DL1-3DS1-2DS4d-3DL2
B20: 3DL3-2DL3-2DP1-2DL1-3DP1(2 copies)-2DL4(2 copies)-3DL1-3DS1-2DS1f-3DL2
2DS4d, the deleted version of 2DS4 (22 bp frameshift deletion); 2DS4f, the full length cell-surface expressed form of 2DS4.